NT

NASA Technical Memorandum 82839

Tribological Characteristics of Nitrogen (N^+) Implanted Iron

(NASA-TM-82839) TRIBOLOGICAL CHARACTERISTICS OF NITROGEN (N+) IMPLANTED IRON (NASA) 24 p HC A02/MF A01 CSCL 11F

N82-24322

Unclas

G3/26 09903

William R. Jones, Jr. and John Ferrante
Lewis Research Center
Cleveland, Ohio

Prepared for the
Joint Lubrication Conference
cosponsored by the American Society of Lubrication Engineers and
the American Society of Mechanical Engineers
Washington, D.C., October 5-7, 1982

NASA

TRIBOLOGICAL CHARACTERISTICS OF NITROGEN (N^+) IMPLANTED IRON

by William R. Jones, Jr. and John Ferrante
National Aeronautics and Space Administration
Lewis Research Center
Cleveland, Ohio

E-1207

ABSTRACT

The effect of implantation of nitrogen ions (1.5 MeV) on the friction and wear characteristics of pure iron sliding against M-50 steel (unimplanted) was studied in a pin-on-disk sliding friction apparatus. Test conditions included room temperature (~25° C), a dry air atmosphere, a load of 1/2 kg (4.9 N), sliding velocities of 0.043 to 0.078 m/sec (~15 to 25 rpm), a pure hydrocarbon lubricant (n-hexadecane), or a U.S.P mineral oil and nitrogen ion implantation doses of 5×10^{15} and 5×10^{17} ions/cm^2.

No differences in wear rates were observed in the low dose (5×10^{15} ions/m^2) experiments. In the high dose experiments (5×10^{17} ions/cm^2), small reductions in initial (~40 percent) and steady-state (~20 percent) wear rates were observed for nitrogen-implanted iron riders as compared with unimplanted controls. No differences in average friction coefficients were noted for either dose.

Auger electron spectroscopy combined with argon ion bombardment revealed a subsurface Gaussian nitrogen distribution with a maximum concentration of 6 atomic percent at a depth of 8×10^{-7} m (0.8 μm). Similar analysis within the wear scar (~2.0×10^{-5} m subsurface) of an implanted rider after 20 μm of wear yielded only background nitrogen concentration. No inward migration of nitrogen ions was observed.

INTRODUCTION

Ion implantation (ref. 1) is the process by which elements are injected into the surface region of a solid. This is accomplished by accelerating ions of the injected element in a vacuum chamber (~10^{-5} torr) and allowing them to strike the solid surface. Ion energies are usually in the range 10 to 500 keV.

The most important application of ion implantation has been in the semiconductor industry to introduce dopants into semiconductors (ref. 2). Other studies have shown that the implantation of certain elements (chromium, helium, and boron) can improve the corrosion resistance of steels and other alloys (refs. 3 to 5). Other applications have been in the areas of catalysis (ref. 6) and fatigue (ref. 7).

A number of investigators have reported substantial reductions in friction and wear of implanted surfaces. Molybdenum and sulfur implanted into the same steel surface reduced friction from 0.26 to 0.20 in unlubricated tests (ref. 8). Implantation of boron, nitrogen, and molybdenum ions reduced wear of nitriding steel by more than a factor of 10 (ref. 9). Similar results were obtained with nitrogen and carbon implanted in several different materials (ref. 10).

More recently, it has become apparent that high nitrogen doses ($>10^{17}$ ions/cm^2) are required to affect the tribological properties of metals (ref. 11). However, the magnitude and direction (moving or stationary member) of these nitrogen implantation effects appear to be quite variable. LoRusso, et al. (ref. 12) reported nitrogen implantation effects on the unlubricated sliding wear of steel. A maximum reduction in the wear rate of 50 percent was observed at a dose of 2×10^{17} ions/cm^2. A higher dose 8×10^{17} ions/cm^2 yielded only a 10 percent wear reduction as compared with unimplanted steel. Hirvonen, et al. (ref. 13) indicate that nitrogen implantation not only reduces wear for stainless steels but also improves the load-carrying capacity, but only under boundary lubricating conditions. However, the life of a tool steel did not improve under milling conditions. Singer, et al. (ref. 14) report large effects (~six times) for titanium implantation in 52100 steel but no effect for nitrogen implantation in abrasive wear tests. The same authors (ref. 15) have reported detrimental nitrogen implantation effects on the abrasive wear resistance of 304 stainless steel.

In contrast, Kirk et al. (ref. 16) in pin-on-disk tests showed that nitrogen implantation ($>10^{17}$ ions/cm^2) yielded large reductions (up to 50 times) in the wear rate of 304 stainless steel disks. However, no wear reductions were observed with 1018 steel.

In general, the effects of ion implantation on wear are unclear. Therefore, the objective of this investigation was to determine the effects of nitrogen implantation (doses of 5×10^{15} and 5×10^{17} ions/cm^2) on the friction and wear properties of pure iron sliding against M-50 steel (unimplanted) using a pin-on-disk apparatus. Other conditions included: a dry air atmosphere, a 1/2 kilogram load (4.9 N), 0.043 to 0.078 meter per second sliding velocity, and a pure hydrocarbon lubricant (n-hexadecane) or a U.S.P. mineral oil.

APPARATUS

The pin-on-disk sliding friction apparatus is shown in figure 1. The test specimens were contained inside a plastic chamber. This allows the moisture content of the test atmosphere to be controlled. A stationary 0.476-centimeter radius hemispherically tipped iron rider was placed in sliding contact with a rotating 6.3-centimeter diameter (1.2 cm thick) steel disk. A constant sliding speed in the range of 0.043 to 0.078 meters per second was maintained. A normal load of 1/2 kilogram (4.9 N) was applied with a deadweight.

MATERIALS

The riders were machined from polycrystalline iron rod (99.95 percent pure) and fully annealed before testing. Some unimplanted riders were tested in the machined state. Others were electropolished. All implanted riders had been electropolished before implantation. The disks were made of CVM M-50 steel with a Rockwell C hardness of 62 to 64. All disks were unimplanted for the wear experiments. One disk was implanted for the Auger spectroscopy experiments. The lubricant for high dose experiments was n-hexadecane with the properties listed in table IA. The n-hexadecane was percolated through alumina and silica gel to remove impurities just before testing. A U.S.P. mineral oil was used for the low dose studies. Its properties appear in table IB.

Specimens were implanted with nitrogen at the State University of New York at Albany. A dynamitron accelerator was used at a beam energy of 1.5 MeV. Beam currents to 20 μA were used. Total doses of $5x10^{15}$ and $5x10^{17}$ ions/cm^2 were attained.

TEST PROCEDURE

Wear Tests

Disk specimens were ground and lapped to a surface finish of $10x10^{-8}$ m R_a. They were then scrubbed with a paste of levigated alumina and water. Riders were cleaned similarly but with a commercial (nonabrasive) detergent instead of alumina. All specimens were dried on clean filter paper.

Approximately 50 milliliters of lubricant was added to the lubricant cup. The chamber was purged with dry air (<50 ppm H_2O) for a minimum of 10 min. The disk was set in motion and the rider loaded against it. Frictional force was measured by a strain gage. Rider wear was determined periodically by stopping the test and measuring the wear scar diameter. Wear rates were then determined for each test and portions of each test by linear regression analysis.

Auger Analysis

To verify that the ion implantation had occurred as expected an Auger electron spectroscopy (AES) depth-profiling analysis was performed on a region of the one nitrogen implanted disk ($5x10^{17}$ ions/cm^2). The depth profile consisted of AES elemental analysis simultaneously with argon ion bombardment. Consequently the distribution of implanted nitrogen with depth could be obtained with high spatial resolution.

The depth profiling was performed in an ultra-high-vacuum system with a base pressure of $1x10^{-10}$ torr. The vacuum system was backfilled with argon to a pressure of $5x10^{-5}$ torr. The surface was then bombarded with a beam of argon ions at a beam energy of 3000 eV and a current density of approximately 20 μA/cm^2 when focused. The beam was rastered, however, over an area of 0.5 cm by 0.5 cm to insure uniformity. In addition, the normal to the analyzed surface was at an angle of 60° to the ion beam direction. The electron beam for AES analysis was centered in the ion-bombarded region and had a beam energy of 2000 eV and beam currents ranging from 1.0 to 5.0 μA depending on the size of the nitrogen AES peak. The beam diameter was nominally $2.5x10^{-5}$ m (25 μm). The surface was then simultaneously sputtered and AES analyzed, with the peak-to-peak height of the nitrogen AES peak determined as a function of time. The sputtering rate was estimated by determining the time needed to sputter through a $1x10^{7}$ m (1000-Å) tantalum oxide film. Since the surface was covered with an oxide and residue lubricant, the nascent surface was taken to be at the point where the low-energy (46 eV) iron peak (ref. 17), saturated (fig. 2).

The sputtering rate estimated from the tantalum oxide film was determined to be 1.4 nm/min. A profilometer trace at the sputtering crater gave good agreement with the calculated depth. This was used to calibrate the depth from the sputtering time. The nitrogen concentration was determined from the relative sensitivities of the 381 eV nitrogen and 703 eV iron peaks (ref. 17). Using this relative sensitivity and the experimental peak-to-peak height ratios (fig. 2) and assuming that the disk was pure iron enabled the atomic concentration of nitrogen with depth to be estimated.

RESULTS - WEAR

Low Dose Experiments

The present authors reported (ref. 18) on the effect of low dose (~5×10^{15} ions/cm^2) nitrogen implantation on the friction and wear properties of pure iron. The conditions of those experiments were the same as the present study except that a U.S.P. mineral oil was used in the former and n-hexadecane in the present work. Table II summarizes the results from the low dose experiments.

The wear rates from table II were essentially the same for the implanted and unimplanted pins. The scatter in the implanted wear rates was much greater than in the unimplanted. Statistical analysis of the wear rates using a student t distribution (ref. 19) indicated that there was no significant statistical difference in wear for these two cases.

High Dose Experiments

Wear

The results of unimplanted control tests for machined iron riders are presented in table III and similar results but with the riders electropolished after machining are given in table IV. Finally, the results for electropolished, nitrogen-implanted iron riders sliding against an unimplanted steel disk are presented in table V. A summary of all the results appears in table VI. Three different wear rates are given in these tables. The initial wear rate refers to measurements taken after the first 2 m of sliding, steady-state wear rate refers to measurements taken after approximately 15 to 150 m of sliding, and the overall wear rate takes all wear measurements into account. Initial wear rates were considered since implantation effects might be magnified in the early wear measurements because of the shallow implantation depth.

As expected, initial wear rates were much higher (by an order of magnitude) than steady-state rates, and the rate variations were greater. Wear (both initial and steady state) appeared to be lower for the electropolished unimplanted rider than for the machined control rider. However, statistical analysis using small sample theory (ref. 19) indicated no significant difference. Similar analyses comparing the initial wear rates for an unimplanted, electropolished rider and a nitrogen-implanted, electropolished rider yielded a difference, significant at a 99-percent confidence level. The same analysis of the steady state rates had a 95-percent confidence level. So the wear rate reductions for nitrogen implantation for initial (~40 percent) and steady state (~20 percent) are statistically valid.

Rider wear volume as a function of sliding distance is plotted in figure 3 for machined unimplanted, electropolished unimplanted, and electropolished nitrogen-implanted riders, respectively. These data have been replotted in a different format in figure 4. Here incremental wear rates between each wear measurement are plotted as a function of sliding distance.

Friction

A typical trace of friction as a function of time is presented in figure 5. All tests, both implanted, and unimplanted, yielded similar traces. All were characterized by an initial friction spike at startup followed by a lower constant value (usually ± 0.005) for the remainder of the test. Values taken from the steady-state portion of the trace are given for each test in tables III to V. The steady-state friction coefficients are averaged in table VI. Essentially, the same value was obtained for all three test series.

Surface Analysis

The results of the AES depth profile (ref. 20) were curve fit to a Gaussian (ref. 21) by linear regression. The equation for the Gaussian is

$$n(x) = n_{max} e^{-(x-x_0)/2\sigma^2} \tag{1}$$

where n is the atomic concentration, x is the depth, x_0 is the range, and σ is the width. The dose can be determined from

$$n_{max} = \frac{\text{dose}}{\sqrt{2\pi}\,\sigma} \qquad \text{(ref. 21)} \tag{2}$$

A typical AES spectrum from the implanted disk is shown in figure 2. The nitrogen AES peak at increased sensitivity is shown in figure 6. The variation in nitrogen concentration with depth is shown in figure 7. The values for the fitting parameter from equation (1) were found to be $x_0 = 8\times10^{-7}$ m (0.8 μm) and $\sigma = 2.2\times10^{-7}$ m (0.22 μm). The value of n_{max} was calculated to be 5.0×10^{21} atoms/cm^3 or approximately 6 atomic percent. The implanted dose as calculated from equation (2) was found to be 2.8×10^{17} atoms/cm^2. The range determined experimentally and analytically by Lang, et al. (ref. 22) for 1.5-MeV nitrogen ions implanted in iron was 8.8×10^{-7} m (0.88 μm), and the experimentally implanted dose was 5.0×10^{17} atoms/cm^2. Considering the various assumptions this agreement indicates that our calibration of depth and concentration was reasonable, and consequently figure 7 gives a good representation of the distribution and concentration of the implanted nitrogen in our wear experiments. Details of the calculation are presented in appendix A.

A further analysis is called for in the present study. Since the riders were hemispherical, the radial distribution of nitrogen across the wear scar was not uniform. This nonuniformity of distribution is analyzed in appendix B. The results of this analysis are presented in figure 8. In that figure the fractional area of the wear scar within a specified depth is shown as a function of the maximum depth at the center of the wear scar. The depths selected were the depth at which the maximum nitrogen distribution occurred to a depth slightly more than this value plus a Gaussian half-width σ. As figure 8 shows, the percentage of the area varies rapidly at first and then varies much more slowly. At a center depth of 10 μm, well beyond the implanted range, approximately 10 percent of the area is still in a region with high nitrogen concentration.

Hardness Measurements

To determine the effects of implantation on hardness, Vickers microhardness measurements were performed on an M-50 disk in implanted (5×10^{17} ions/cm^2) and unimplanted regions in a separate experiment. A load was used with an average penetration depth of approximately 2 to 3 μm. This samples the implanted region, which has a maximum dose at ~1 μm. The results were average hardnesses of 996 ± 35 kg/mm^2 in the implanted region and 821 ± 38 kg/mm^2 in the unimplanted region, an indication of increased hardness due to implantation.

DISCUSSION

Using pin wear to determine the effects of ion implantation is quite a severe test. In the initial stages of the test (e.g., ~2 m of sliding distance) the depth worn at the center of the wear scar (~5 μm) was well beyond the implanted range. Although this depth varied with radial position, a large fraction of the contact region was beyond the range of the implantation. Consequently in this study a relatively high implantation energy (1.5 MeV) was selected to give a large range (~1 μm). In other current studies, much lower energies are being used (~50 keV with ranges of 0.1 to 0.2 μm). In all these studies, effects well beyond the implantation range have been observed. Generally, inward diffusion of the implanted species during the wear process is offered as an explanation for the exceptional depths of effectiveness (ref. 11). Our observations also indicated decreased wear well beyond the implantation range. Effects are still seen in the mild wear range, where final wear depth on the pin is about 20 μm. However, in light of the analysis presented in appendix B and figure 8 these results can be understood simply in terms of the geometry of the contact. A fraction of the area comparable to wear reduction still is within the implantation range. Thus there is no strong evidence for effects beyond the implantation range. Auger analysis of these final wear scars revealed no significant nitrogen concentration near the center of the scars, that is, no higher than was observed by Jones and Ferrante (ref. 18), where a null result was obtained. The extended range of effectiveness in the other studies may be due to strain fields resulting from the implantation but well beyond the range of the implanted ions. However, implantation with argon (ref. 23) showed no improvement.

Bolster and Singer (ref. 15) observed a reduction in abrasive wear in a carbon steel and an increase in wear in 304 stainless steel. Bolster and Singer performed one of the few studies where repeatability was checked. However, even in their elegant studies the scatter was such that at times no effect was observed at approximately the same conditions. Hartley (ref. 11) attributes the improved wear resistance of ferrous materials to a formation of martensitic structures with the nitrogen. Most studies to date have been performed on alloys, which are complicated combinations of materials. The fact that a positive result is found in pure iron should help sort out mechanisms concerning minor components in alloys. For example, the nitrogen could be interacting with the iron to produce martensitic hardening (ref. 11) without worry about what other interactions may be taking place with other alloy components. In iron chromium alloys, chemical interaction of nitrogen with chromium rather than with iron would be far more likely because chromium nitrides have a higher free energy of formation than iron nitrides. However, for similar reasons nitrogen should diffuse more readily in iron.

A final point of interest is which component shows an effect in a sliding or rolling contact. Hirvonen, et al. (ref. 23) observed no effect on wear in the stationary component in a crossed-cylinders configuration. This would not necessarily be surprising, since in this case the stationary component undergoes constant wear. With low implantation energies the range of implantation is only of the order of 0.1 μm and could be expected to wear away quickly even with an enhanced depth of effectiveness. Surprisingly, Hirvonen found that implantation of the rotating component decreases wear in the stationary component. In the present study a decrease in wear of the stationary component (the rider, which is undergoing continuous wear) was observed. This was probably due to our greater depth of implantation. Consequently a wear reduction on the member undergoing continuous wear in a sliding configuration was observed.

As indicated, a number of interesting experiments have been done concerning the effects of ion implantation on wear. To date, however, there is no clear-cut understanding of the physical mechanisms involved. Therefore effort now should be directed toward designing experiments that would clarify these mechanisms.

SUMMARY OF RESULTS

A sliding pin-on-disk apparatus was used to determine the effect of nitrogen ion implantation on the friction and wear characteristics of pure iron sliding against M-50 steel. The major results were as follows:

1. No differences in wear rates were observed in low dose ($5x10^{15}$ ions/cm^2) experiments.

2. In high dose ($5x10^{17}$ ions/cm^2) experiments, small reductions were effected in initial (~40 percent) and steady-state (~20 percent) wear rates of nitrogen implanted iron riders.

3. Average friction coefficients were not affected by nitrogen ion implantation at either dose.

4. A Gaussian nitrogen distribution with a maximum concentration of ~6 atomic percent at a depth of $8x10^{-7}$ m (0.8 μm) was observed in an unworn, implanted disk by Auger electron spectroscopy (AES).

5. AES revealed only background nitrogen concentration within the wear scar of an implanted rider. No inward migration of nitrogen ions was observed.

6. The present results can be understood simply in terms of a geometrical analysis of the pin-on-disk configuration and not in terms of any effect beyond the range of implantation.

APPENDIX A
CALIBRATION OF DEPTH OF IMPLANTATION AND CONCENTRATION OF IMPLANTED NITROGEN

The first step in the calibrations was to obtain the relative AES sensitivities for the 703-eV iron peak and the nitrogen peak from the PHI handbook (ref. 17), giving $(N/Fe)_1 = 1.64$. The equivalent ratio of AES peak heights was then obtained by ratioing the nitrogen to iron AES peaks at the maximum in the Gaussian distribution curve, giving $(N/Fe)_2 = 0.103$. The quotient then is the actual atomic ratio of nitrogen to iron.

$$\frac{N}{Fe} = \left(\frac{N}{Fe}\right)_2 \Big/ \left(\frac{N}{Fe}\right)_1 = 0.0628$$

Assuming the total adds to unity, $N + Fe = 1$. Solving these equations simultaneously gives $N = 0.059$, or 5.9 atomic percent. Therefore nitrogen has a concentration of approximately 6 atomic percent at the maximum.

Next we can estimate the implanted dose from our curve fit to a Gaussian (ref. 21)

$$n_{max} = \frac{\text{dose}}{\sqrt{2\pi}\ \sigma} \tag{1}$$

As an approximation we assume that the atomic density of the implanted region is the same as that of body-centered cubic iron (8.49×10^{22} atoms/cm^3). Therefore $n_{max} = (0.059)\ (8.49 \times 10^{22}$ atoms/cm$^3) = 5.01 \times 10^{21}$ atoms/cm^3. We obtain σ from the curve fit to the Gaussian, where $\sigma = 2.19 \times 10^{5}$ cm; and thus from equation (1)

$$\text{dose} = \sqrt{2\pi}(5.01 \times 10^{21}\ \text{atoms/cm}^3) \times (2.19 \times 10^{-5}\ \text{cm}) = 2.8 \times 10^{17}\ \text{atoms/cm}^2$$

which is in agreement with the implanted dose (5×10^{17} ions/cm^2) and which independently indicates that the sputtering depth calibration is reasonable.

APPENDIX B

HEIGHT REMOVED AS A FUNCTION OF RADIAL POSITION ON THE WEAR SCAR

where

A	area of wear scar
ΔA	implanted area
h	maximum height removed at center of wear scar
h'	height removed at r'
R	radius of rider
r	radius of wear scar
r'	radial position on wear scar

By applying some simple geometry and trigonometry we can derive the desired relation. From the law of Cosines, on triangle BCD

Side view　　　　Top view

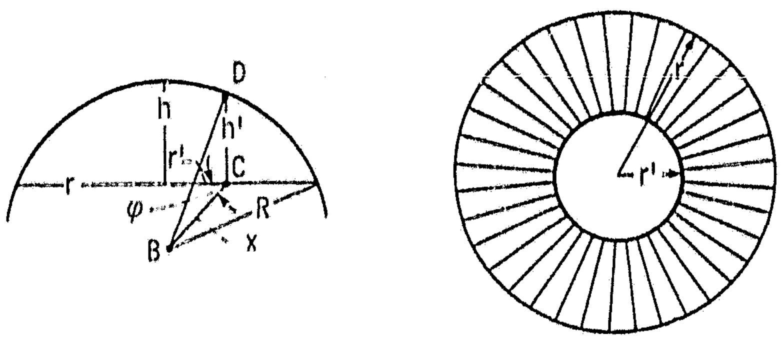

$$R^2 = h'^2 + X^2 - 2h' X \cos \theta \tag{B1}$$

(θ is defined by the angle BCD, where

$$\theta = 90^\circ + \phi$$

$$X = \sqrt{(R - h)^2 + r'^2} \tag{B2}$$

$$\sin \phi = \frac{R - h}{X} \tag{B3}$$

$$h = R - \sqrt{R^2 - r^2} \tag{B4}$$

Substituting into equation (B1) and rearranging gives

$$r'^2 = R^2 - h'^2 - (R - h)^2 - 2h'(R - h) \tag{B5}$$

Finally

$$\frac{\Delta A}{A} = \frac{r^2 - r'^2}{r^2} = 1 - \left(\frac{r'}{r}\right)^2 \tag{B4}$$

Therefore, from equations (B4) and (B5) we can calculate $\Delta A/A$ as a function of h, with h' as a parameter (fig. 8).

REFERENCES

1. Townsend, Peter D.; Kelly, J.C.; and Hartley, N.E.W.: Ion Implantation, Sputtering, and Their Applications. Academic Press (London), 1976.
2. Mayer, James, W.; Erickson, Lennart; and Davies, John A.: Ion Implantation in Semiconductors, Academic Press, 1970.
3. Ashworth, V.; et. al.: Effect of Ion Implantation on the Corrosion Behavior of Iron. Ion Implantation in Semiconductors and Other Materials, S. Namba, ed., Plenum Press, 1975, pp. 367-373.
4. Khirnyi, Yu M.; and Solodovnikov, A.P.: Effect of Increased Corrosion Resistance in Metals Irradiated with Helium Ions. Sov. Phys. Dokl., vol. 19, 1974, p. 31.
5. Rickards, J.; and Dearnaley, G.: Ion Implantation and Backscattering from Oxidized Single-Crystal Copper. Applications of Ion Beams to Metals, S.T. Picraux, E.P. Eernisse, and F.L. Vook, eds. Plenum Press, 1974, pp. 101-109.
6. Grenness, M.; Thompson, M.W.; and Cahn, R.W.: J. Appl. Electrochem. vol. 4, no. 3, 1974, pp. 211-218.
7. Hartley, N.E.W.: Tribological Effects in Ion-Implanted Metals. Inst. Phys. Conf. Ser. No. 28, 1976, Ch. 5, pp. 210-223.
8. Hartley, N.E.W.; Dearnaley, G.; and Turner, J.F.: Frictional Changes Induced by the Ion Implantation of Steel. Ion Implantation in Semiconductors and Other Materials, B.L. Crowder, ed., Plenum Press, 1973, pp. 423-436.
9. Picraux, S.T.; Eernisse, E.P.; and Vook, F.L., eds.: Application of Ion Beams to Metals. Plenum Press, 1974, p. 123.
10. Hartley, N.E.W.: Ion Implantation Case Studies - Manufacturing Applications. Paper presented at the Institution of Metallurgists Spring Review Course, "Surface Treatments for Protection", University College, Cardiff, April 7-10, 1978.
11. Hartley, N.E.W.: Friction and Wear of Ion-Implanted Metals - A Review. Thin Solid Films, 64 (1979), pp. 177-190.
12. LoRusso, S.; Mazzoldi, P.; Scotoni I.; Tosello, C.; and Tosto, S.: Effect of Nitrogen-ion Implantation on the Unlubricated Sliding Wear of Steel. Appl. Phys. Litt. 34(10), (1979), pp. 627-629.
13. Hirvonen, J.K.; Carosella, C.A.; Kant, R.A.; Singer, L.; Vardiman, R.; and Rath, B.B.: Improvement of Metal Properties by Ion Implantation. Thin Solid Films, 63, (1979), pp. 5-10.
14. Singer, I.L.; Bolster, R.N.; and Carosella, C.A.: Abrasive Wear Resistance of Ti- and N-Implanted 52100 Steel Surfaces. Thin Solid Films 73, (1980), pp. 283-289.
15. Bolster, R.N.; and Singer, I.L.: Surface Hardness and Abrasive Wear Resistance of Ion-Implanted Steels. ASLE TRANS, 24, 4 (1981), pp. 526-532.
16. Kirk, J.A.; Egerton, G.W.; and Sartwell, B.D.: "Wear and Friction of Nitrogen Ion Implanted Steel", presented at ASLE/ASME Joint Lubrication Conference, New Orleans, LA, Oct. 4-7, 1981.
17. Palmberg, P.W.; Riach, G.E.; Weber, R.E.; and MacDonald, N.C.: Handbook of Auger Spectroscopy, Physical Electronics Industries, Edina, MN, (1972).
18. Jones, William R. Jr.; and Ferrante, John: The Effect of Nitrogen Ion (N^+) Implantation on the Friction and Wear Characteristics of Iron. NASA TM 79029, 1978.

19. Spiegel, Murray R.: Schaum's Outline of Theory and Problems of Statistics, Statistics. Schaum Publishing Co., 1961.
20. Ferrante, John: Practical Applications of Surface Analysis in Tribology. NASA-TM-8184, 1980. Presented at the International Lubrication Conference, ASME-ASLE, San Francisco, Aug. 18-21.
21. Wilson, R.G.; and Brewer, G.R.: Ion Beams with Applications to Ion Implantation, Wiley Interscience, John Wiley and Sons, New York, 1973, pp. 270-284.
22. Land, D.J.; Simons, D.G.; Brennan, J.G.; and Brown, M.D.: Z_2 and Energy Dependence of Range Distributions and Stopping Power for Nitrogen in Solids. Phys. Rev. A, vol. 22, p. 68 (1980).
23. Hirvonen, J.K.: Ion Implantation in Tribology and Corrosion Science. J. Vac. Sci. Technol., vol. 15, no. 5, Sep.-Oct., 1978, pp. 1662-1668.

TABLE IA. - TYPICAL PROPERTIES OF LUBRICANT n-HEXADECANE AT 20° C

[High dose (5×10^{17} ions/cm^2) experiments]

Viscosity, cP	3.34
Density, g/milliliter	0.775

TABLE IB. - TYPICAL LUBRICANT PROPERTIES

[Low dose (5×10^{15} ions/cm^2) experiments (ref. 18).]

Lubricant type	U.S.P. mineral oil
Viscosity, cP	
37.8° C	60
98.9° C	7
Specific gravity	
15.6° C	0.888
25° C	0.883

TABLE II. - SUMMARY OF FRICTION AND WEAR RESULTS FROM LOW DOSE NITROGEN IMPLANTATION EXPERIMENTS (REF. 18)

Implanation species	Number of tests	Average coefficient of friction	Average wear rate $M^3/N\text{-}M \times 10^{-14}$	Standard deviation
None	6	0.10	1.47	±0.27
Nitrogen[a]	8	.09	1.53	±0.73

[a]5×10^{15} ions/cm^2.

ORIGINAL PAGE IS
OF POOR QUALITY

TABLE III. – FRICTION AND WEAR RESULTS FOR UNIMPLANTED, MACHINED IRON RIDER

[Unimplanted M-50 steel disk; 4.9-N load.]

Test	Sliding velocity, m/sec	Steady-state friction coefficient	Initial	Steady state	Overall
			Wear rate, $m^3/N \cdot m$		
1	0.072	0.14	58×10^{-15}	5.7×10^{-15}	7.6×10^{-15}
2	.067	.15	79	6.2	8.0
3	.077	.14	57	9.3	10.0
4	.070	.15	36	5.7	6.2
5	.069	.15	45	3.6	4.4
6	.075	.15	30	4.4	5.0
7	.072	.14	60	7.7	9.9
8	.071	.15	71	10.0	11.0

TABLE IV. – FRICTION AND WEAR RESULTS FOR UNIMPLANTED, ELECTROPOLISHED IRON RIDER

[Unimplanted M-50 steel disk; 4.9-N load.]

Test	Sliding velocity, m/sec	Steady-state friction coefficient	Initial	Steady state	Overall
			Wear rate, $m^3/N \cdot m$		
9	0.073	0.15	42×10^{-15}	3.7×10^{-15}	4.9×10^{-15}
10	.078	.14	37	4.0	4.7
11	.078	.16	42	4.6	5.7
12	.075	.16	44	6.1	7.5
13	.071	.14	45	6.0	7.5

TABLE V. – FRICTION AND WEAR RESULTS FOR NITROGEN-IMPLANTED, ELECTROPOLISHED IRON RIDER[a]

[Unimplanted M-50 steel disk; 4.9-N load.]

Test	Sliding velocity, m/sec	Steady-state friction coefficient	Initial	Steady state	Overall
			Wear rate, $m^3/N \cdot m$		
14	0.078	0.15	18×10^{-15}	2.1×10^{-15}	2.8×10^{-15}
15	.075	.15	20	2.8	3.7
16	.073	.15	57	3.2	4.0
17	.078	.16	33	4.4	5.4
18	.074	.15	34	5.0	6.6
19	.071	.15	30	4.2	5.3
20	.070	.15	37	5.5	6.6

[a] 5×10^{17} ions/cm^2.

ORIGINAL PAGE
BLACK AND WHITE PHOTOGRAPH

TABLE VI. - SUMMARY OF FRICTION AND WEAR TESTS

Rider preparation	Initial	Steady state	Overall	Average friction coefficient
	Wear rate, $m^3/N{\cdot}m$			
Unimplanted, machined rider	$55\times10^{-15}\pm17^a$	$6.5\times10^{-15}\pm2.3^a$	$6.9\times10^{-15}\pm2.2^a$	0.15 ± 0.005^a
Unimplanted, electropolished rider	43 ± 5.1^a	4.9 ± 1.1^a	5.4 ± 1.3^a	0.15 ± 0.01^a
Nitrogen-implanted,[b] electropolished rider	27 ± 8.4^a	3.9 ± 1.2^a	4.4 ± 1.3^a	0.15 ± 0.004^a

[a]Standard deviation.
[b]5×10^{17} ions/cm^2.

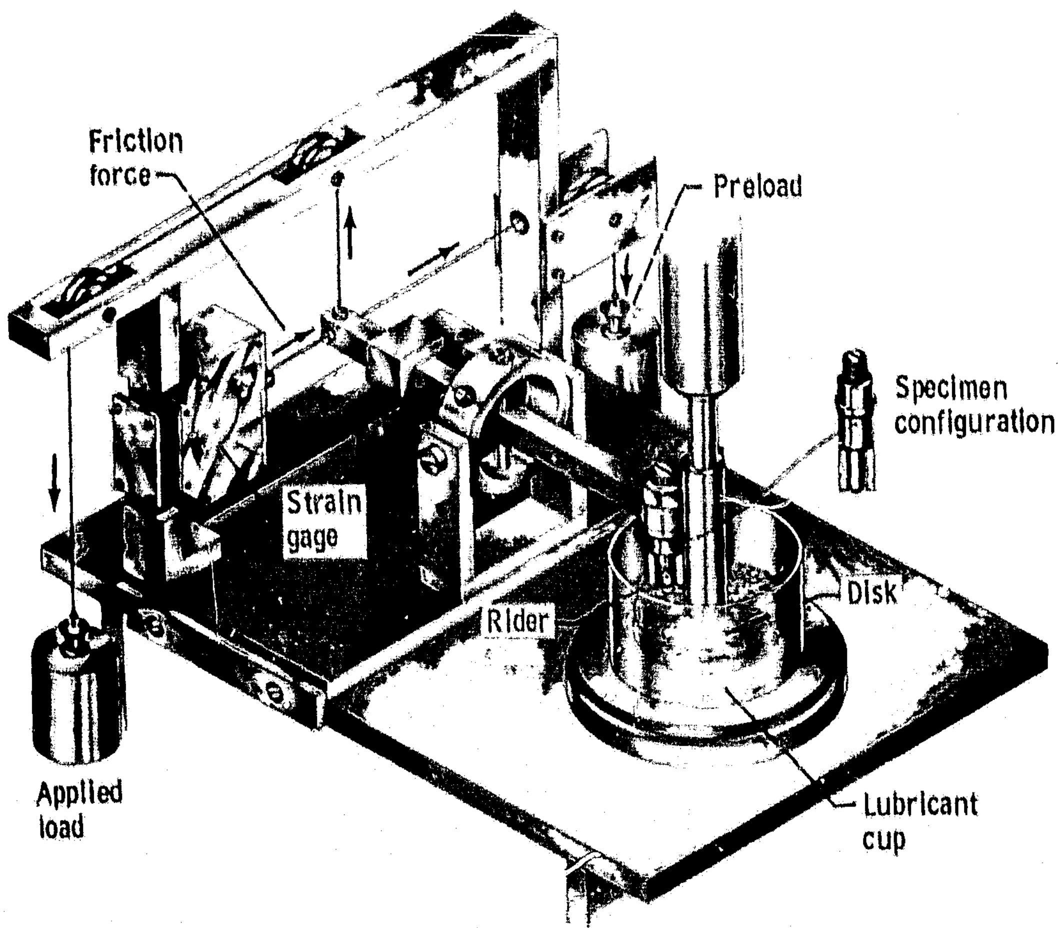

Figure 1. - Pin-on-disk sliding friction apparatus.

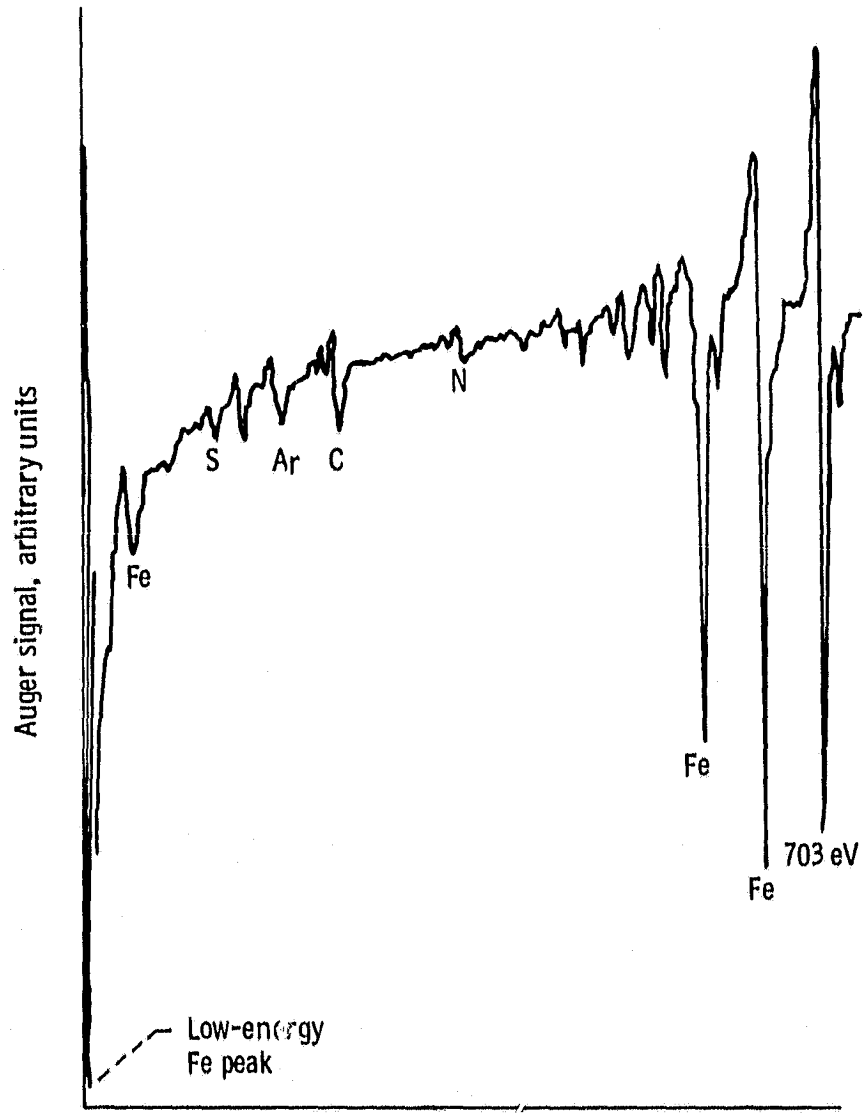

Figure 2. - Auger spectrum of nitrogen-implanted M-50 steel disk surface after 660 minutes of sputtering (~750 nm).

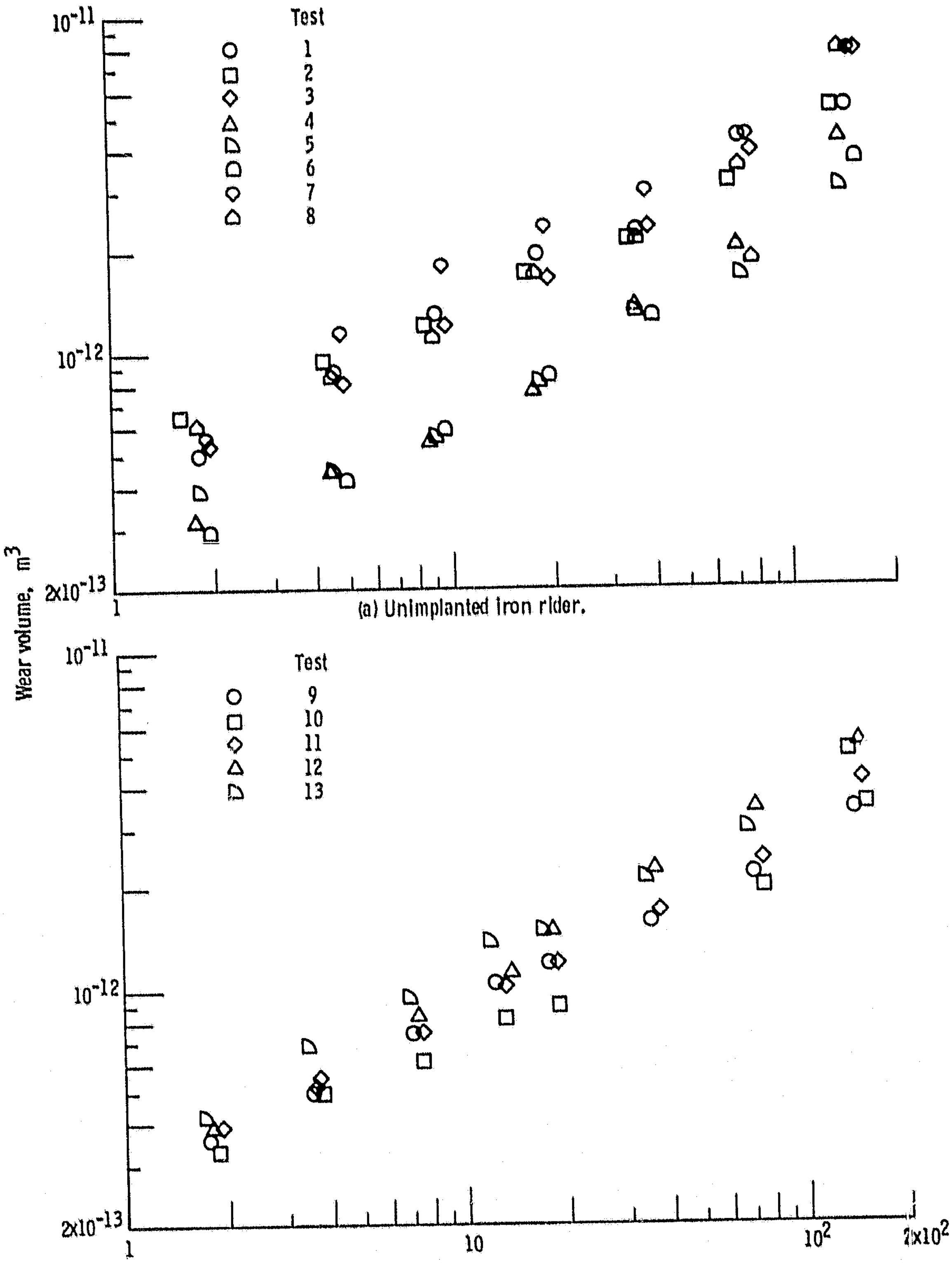

(b) Unimplanted, electropolished iron rider.

Figure 3. - Rider wear volume as a function of sliding distance. Load, 4.9 N; sliding velocity ~0.07 m/sec; lubricant, n-hexadecane; disk, unimplanted M-50 steel.

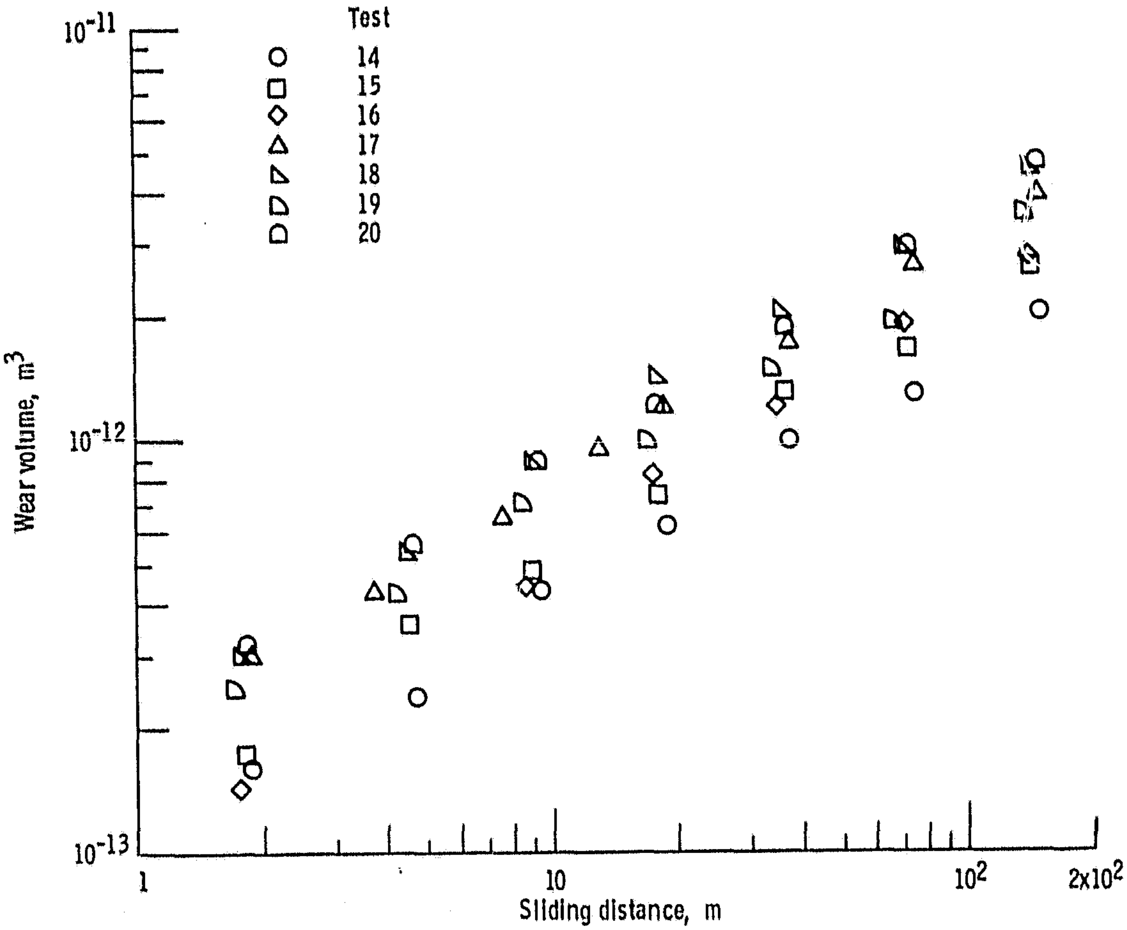

(c) Nitrogen-implanted, electropolished iron rider.

Figure 3. - Concluded.

ORIGINAL PAGE IS
OF POOR QUALITY

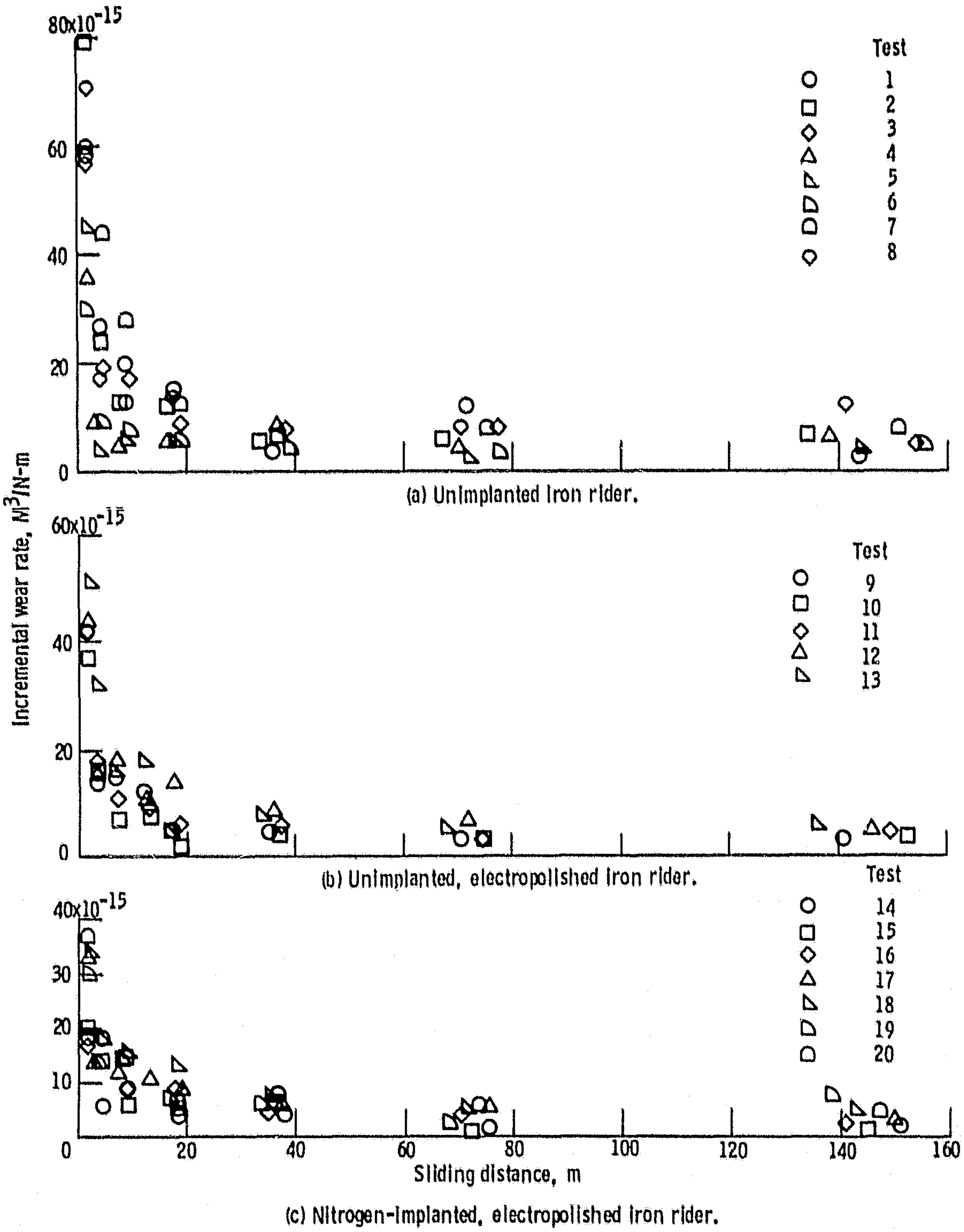

Figure 4. - Incremental wear rate as a function of sliding distance. Load, 4.9 N; sliding velocity, ~0.07 m/sec; lubricant, n-hexadecane; disk, unimplanted M-50 steel.

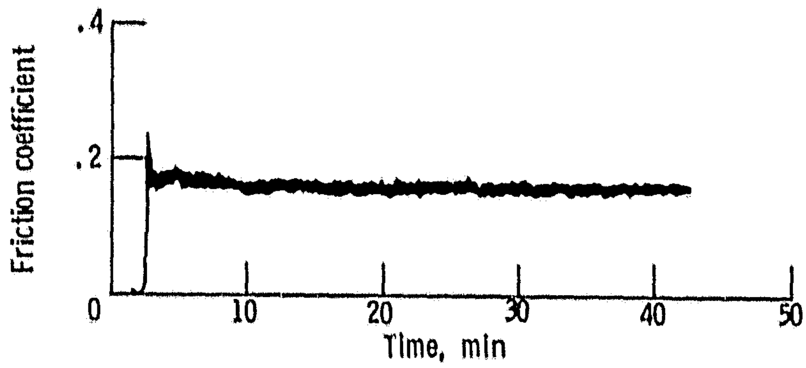

Figure 5. - Typical friction-time trace.

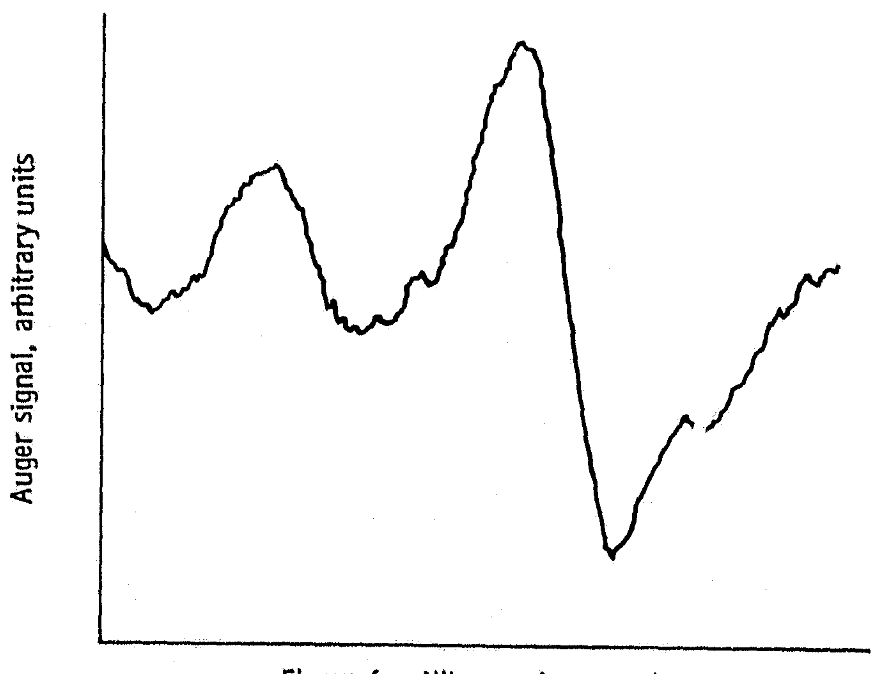

Figure 6. - Nitrogen Auger peak.

ORIGINAL PAGE IS
OF POOR QUALITY

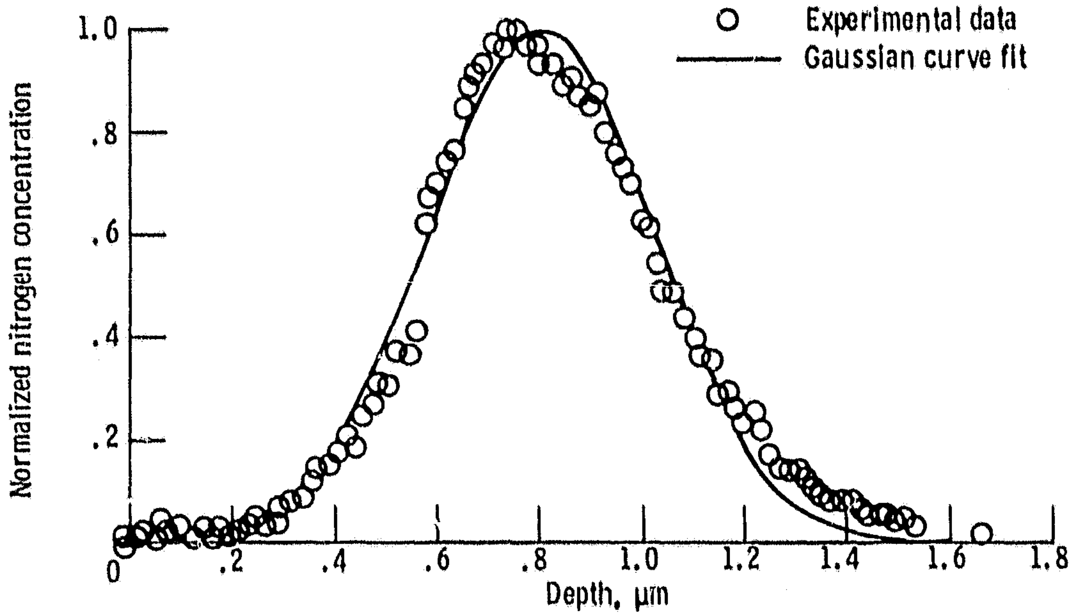

Figure 7. - Nitrogen concentration as a function of depth in nitrogen-implanted steel disk.

ORIGINAL PAGE IS
OF POOR QUALITY

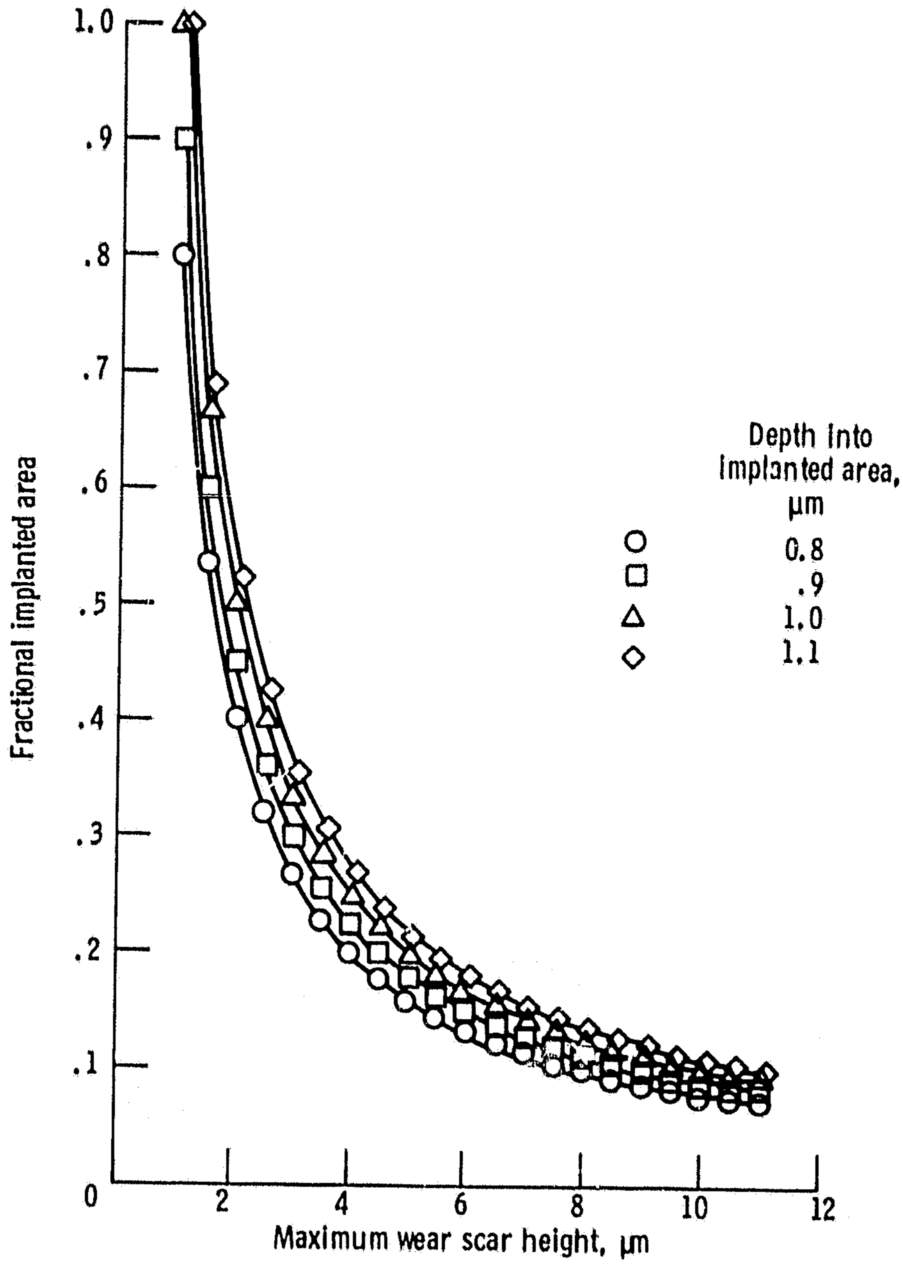

Figure 8. - Fractional implanted area as a function of maximum wear scar height.